DEMONSTRATION TOKAMAK POWER PLANT

M. Abdou, C. Baker, J. Brooks, D. Ehst, R. Mattas, and D. Smith
Fusion Power Program, Argonne National Laboratory
9700 S. Cass Ave., Argonne, IL 60439
(312) 972-4835

D. DeFreece, G. D. Morgan, and C. Trachsel
McDonnell Douglas Astronautics Company
P.O. Box 516, Bldg. 81/2, St. Louis, MO 63166
(314) 576-8274

ABSTRACT

A conceptual design for a tokamak demonstration power plant (DEMO) was developed. A large part of the study focused on examining the key issues and identifying the R&D needs for: 1) current drive for steady-state operation, 2) impurity control and exhaust, 3) tritium breeding blanket, and 4) reactor configuration and maintenance. Impurity control and exhaust will not be covered in this paper but is discussed in another paper in these proceedings, entitled "Key Issues of FED/INTOR Impurity Control System".

I. INTRODUCTION

The basic goal of this study was to provide a technical perspective and conceptual design of a tokamak demonstration power plant (DEMO). The effort was focused on designing the key features of such a device with the objective of providing design information for guiding the research and development efforts. While a reference conceptual design was developed, less emphasis was placed on a single point and more emphasis was placed on exploring major design features. The results of the study are detailed in Ref. 1. The study was carried out by the STARFIRE team.[2]

II. REACTOR PARAMETERS AND CONFIGURATION

Table 1 shows the major parameters for the DEMO. The configuration selected for the DEMO is shown in Fig. 1. Dominant features of the configuration are the flat top on the reactor, which was chosen to minimize the reactor building height; the single sector per TF coil ; and the combined vacuum boundary with sector sealing near the outer leg of the TF coil. No intertwined superconducting coils are used and four sets of redundant vacuum pumps are located in the basement.

TABLE 1. DEMO MAJOR PARAMETERS

Net Elec. Power, MWe	330
Gross Elec. Power, MWe	385
Fusion Power, MW	1069
Thermal Power, MW	1138
Gross Turbine Eff., %	33.6
Overall Availability, %	50
Avg. Neutron Wall Load, MW/m^2	2.1
Major Radius, m	5.2
Plasma Half-Width, m	1.3
Plasma Elongation (b/a)	1.6
Inboard Blanket/Shield Thick. m	1.2
Plasma Current, MA	8.7
Avg. Toroidal Beta	0.075
Toroidal Field on Axis, T	4.8
Maximum Toroidal Field, T	10
Number of TF Coils	8
Plasma Burn Mode	Continuous
Plasma Heating Method	*
Current Drive Method	*
Impurity Control	Pumped Limiter
Tritium Breeder	Li_2O (or $Li_{17}Pb_{83}$)
Breeding Ratio, Net	1.05
Max. Component Wt (TF Coil), Mg	440
EF Coil Sys. Stored Energy, GJ	5.7
TF Coil Sys. Stored Energy, GJ	20

*Relativistic Electron Beam.

A major area of uncertainty for future demonstration and commercial fusion reactors is achieving the availability goal, which is dependent on component outage rate (reliability and lifetime) and on the outage time for maintenance. Therefore, the DEMO design features were selected and developed to enhance reliability and minimize replacement time. The most important design feature selected to enhance reliability is steady-state plasma operation, which reduces cyclic loading and

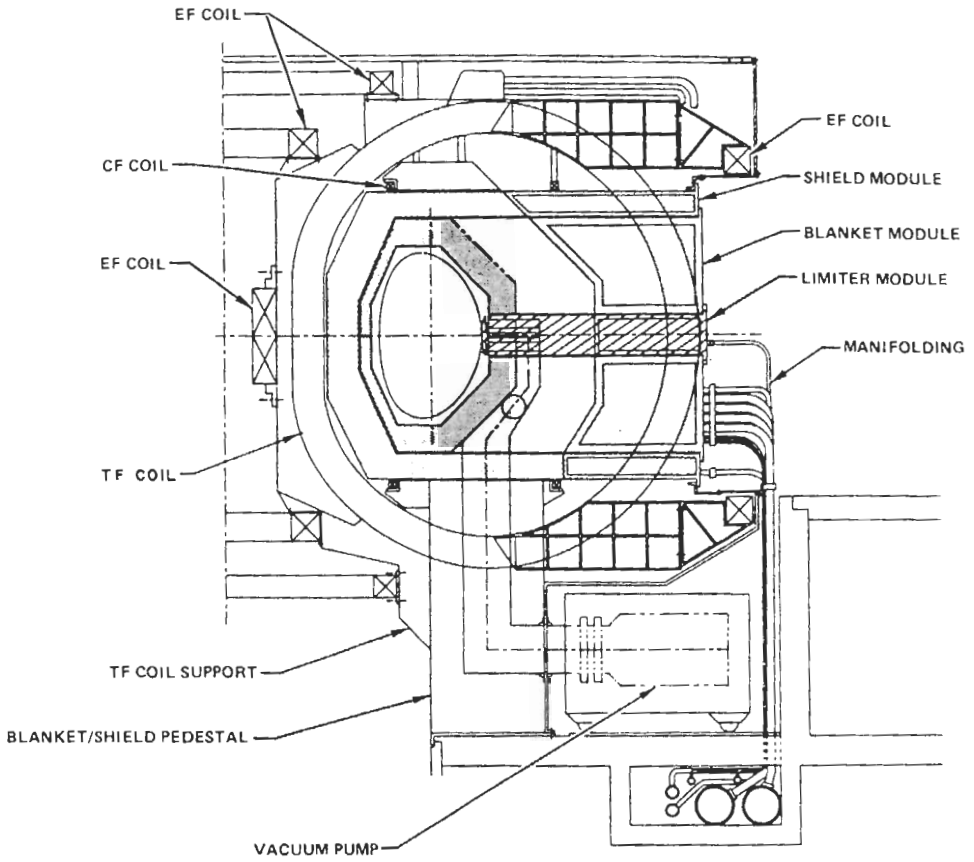

Figure 1. Vertical cross section of DEMO reference design.

minimizes the number of plasma disruptions. Another important aspect in the DEMO is that availability will be improved by striving for reactor simplicity. Since the STARFIRE study, the INTOR group[3] has shown the feasibility of utilizing a 4°K anti-torque structure, which greatly improves access to the reactor. This feature was incorporated into the DEMO design.

The DEMO reactor design was further simplified by reducing the number of components and connections, simplifying sealing surface geometry, and combining components to reduce the number of maintenance operations required (saves time) and decrease complexity (improves reliability). The major configuration features that lead to reactor simplification are: a) a 4°K segmented anti-torque structure, b) one limiter/blanket/shield sector per TF coil, c) eight TF coils, and d) a combined TF coil and plasma boundary These features have resulted in a decrease in the number of major parts by a factor of two from the STARFIRE configuration and reduced the number of major seals and connections by a factor of four. These changes reduce the replacement time by approximately a factor of two and increase the blanket system reliability by as much as a factor of four (if connections dominate the reliability, as expected).

Choice of a single, blanket/shield/ limiter sector per TF coil results in the need for a larger TF coil outer leg radius so that adequate access is provided for single sector installation. The outer leg radius and peak-to-peak field ripple are 11.6 m and 3.5% for 8 coils, 12 m and 1.1% for 10 coils, and 12.3 m and 0.3% for 12 coils. Eight TF coils were chosen because the number of blanket/shield/ limiter sectors is proportional to the number of TF coils, and thus the number of connections and major components is reduced thereby further reducing replacement time and increasing reliability.

The decision of one sector per TF coil increased the requirements for TF coil size and, consequently, the stored energy in the EF coil system and the reactor building size. These effects were evaluated to determine the

increased capital costs. A study of the EF coil stored energy indicated that the major benefit could be obtained by decreasing the TF coil height (~ 6 GJ/m), as opposed to decreasing the TF coil radius (~ 0.5 GJ/m). As a result, a curvature-supported TF coil shape was selected in place of the conventional coil shape. The curvature-supported coil requires an extension of the center post at the top and bottom of the coil inner leg to maintain a minimum bending coil. The building height was not affected by the coil radius change and the additional costs for building width was ~ $10M. These costs are not considered excessive compared to the benefits derived in availability.

Simplified TF coil replacement was achieved by eliminating the need for a common vacuum tank around the inner legs of the TF coils and by adopting the 4°K anti-torque structure of INTOR. It was found that, if the basic vacuum boundary was moved to the exterior of all TF and EF coils and the shield sectors were inserted through this boundary and sealed together under each TF coil, then separate vacuum boundaries could be provided for the plasma and TF coils using all planar seals. These seals are inherently simpler to replace than the structural joints used in the common vacuum tank of previous designs, where structural welds had to be cut and remade. Dual seals with intermediate vacuum pumping between shield sectors limit tritium leakage. Additionally, the 4°K anti-torque structure was segmented with a clevis joint equidistant between the coils to permit carrying the overturning load without structural welding. This segmentation permits radial coil removal after the blanket and shield sectors, outer EF coils, and the outer vacuum wall panel are removed. Another major benefit of the combined vacuum boundary is that it eliminates the need for an additional structural boundary between the TF coils and the shield. This results in eliminating ~ 8 cm of radial build in the inner blanket/shield and could result in capital cost savings of ~ $50M. Yet another benefit of the combined vacuum boundary is that all magnetic loads in the 4°K structure can be reacted without additional thermal isolation. The large outer EF coils are supported by the 4°K TF coils, and the inner EF coils are supported by the center post.

TF coil replacement is accomplished by removing the blanket/shield sectors on either side of the coil, removing the outer EF coils and vacuum tank rings, cutting the outer wall panel and extracting the coil radially. It is estimated that TF coil replacement can be achieved in less than six months using remote maintenance with this approach. This represents an improvement of a factor of at least two over previous designs.

The DEMO total direct cost for the complete reactor plant is 1.52 billion dollars. Adding in the indirect and escalation costs during construction brings the total to 2.35 billion dollars. The largest single cost account is the Reactor Plant Equipment which represents 50% of the plant cost.

III. TRITIUM BREEDING BLANKET

The DEMO study focused on the definition of materials and design issues for first wall/blanket concepts using two different breeders: (1) solid lithium oxide (Li_2O) and; (2) a liquid metal, the lead-rich Li-Pb eutectic (17 at. % Li, 83 at. % Pb).

A. Li_2O breeder blanket concept

Pressurized water (260-300°C) was selected for the first wall and blanket coolant. The range of operating temperatures required for acceptable Li_2O performance is very limited, and thus the low ΔT characteristic of pressurized water systems appears necessary for a satisfactory design. Compared to helium coolant, water coolant permits a smaller reactor size or a higher fusion power provides for much lower pumping power losses, and results in lower cost of the heat transport system. An advanced austenitic stainless steel (designated PCA), similar to Type 316, was selected as the structural material. Mechanical properties and radiation damage resistance are considered acceptable for reasonable lifetimes (~ 7 MW-yr/m^2) at the relatively low projected operating temperatures, which are below the temperatures at which severe displacement damage embrittlement, helium embrittlement, and maximum swelling occur.

The 1-D neutronics calculations indicate that, in the absence of a neutron multiplier, the tritium breeding potential of a Li_2O blanket decreases significantly with ^6Li enrichment of natural lithium. The maximum breeding ratio (100% blanket) is 1.23 for a Li_2O blanket with a stainless steel first wall and armor 13.4-mm thick. However, the net breeding ratio (3-D) is only ~ 1.05 with no inboard blanket. Beryllium was found to be the only effective neutron multiplier for a Li_2O blanket. The beryllium multiplier is more effective when placed behind several centimeters of Li_2O.

Tritium recovery is considered to be a key feasibility issue for Li_2O as a tritium breeder material. Tritium generated within the Li_2O grains must diffuse to the surface of the grains, desorb as T_2O, migrate through interconnected porosity to a helium purge stream, and convect to the tritium processing system. Similar to the case for STARFIRE, a Li_2O microstructure with small grain size ($\lesssim$ 1 μm) and a bimodal pore distribution is believed to offer the greatest potential for acceptable tritium recovery. The difficult design problems arise from the limited operating temperature range projected for Li_2O and the relatively low thermal conductivity (about 2 W/m-K for irradiated material at 70% of theoretical density). Effects that result in a projected allowable operating temperature range between 410 and 670°C for Li_2O are summarized in Table 2. The critical concerns relate to the fact that some of the phenomena may cause irreversible propagating-type effects. For example, precipitation of LiOT could lead to enhanced sintering at low temperatures, which, in turn, would produce higher tritium partial pressures and, hence, more LiOT precipitation and subsequently more sintering. Mass transport of LiOT leads not only to a loss of lithium from the blanket but also to possible corrosion problems caused by precipitation of liquid LiOT in the tritium processing circuit. Analyses indicate that, in the absence of radiation effects, the blanket tritium inventory can be maintained at relatively low levels (< 50 g in Li_2O). However, radiation effects are expected to substantially increase the tritium inventory, possibly to unacceptable levels.

TABLE 2. BASIS FOR ALLOWABLE OPERATING TEMPERATURE RANGE OF Li_2O

Maximum Allowable Temperature .	
Radiation-induced sintering	700°C
Mass Transport of LiOH (1% of T_2O)	670°C
Minimum Allowable Temperature	
Solid state diffusion (1 μm grain)	410°C
LiOT precipitation (160 Pa)	410°C

Materials compatibility issues include breeder-structure, coolant-structure and breeder-coolant compatibility. The first two issues involve normal operation whereas breeder-coolant compatibility is of interest only in the event of off-normal conditions such as a coolant leak into the breeder region. Limited data from short-term sealed capsule experiments indicate that the reactivity of Li_2O with stainless steel is probably not excessive. However, no data exist under the more severe conditions of appropriate oxygen and moisture pressures.

Thermal-hydraulics analyses were conducted to evaluate the sensitivity of the blanket design, particularly with respect to tritium recovery, to variations in breeder physical properties, geometrical parameters, and reactor power level. The results indicated that the tolerances required for adequate predictability of heat transfer through a helium gap at the breeder-to-coolant-tube interface were too small for practical systems. A different design concept, which has been considered for the interface, consists of a commercial stainless steel metallic felt between the breeder and tube. The thermal conductance of the interface can be adjusted by varying the thickness and density of the felt. Compatibility with the breeder (Li_2O is a major concern in this concept. The blanket was also analyzed to determine the design changes necessary to accommodate deliberate large-scale changes in reactor power level. A power factor change of 2 could potentially be accommodated by making design detail changes, which would result in a reduction of ~ 0.08 in tritium breeding ratio.

Thermal stress analyses of the Li_2O breeder were conducted to determine the breeder's propensity to fracture under operational thermal gradients (410°C to 660°C radially outward from the breeder cylinder's central coolant tube, for cylinder diameters of 2 to 6 cm). Circumferential and axial peak stresses in the cylinder were higher by factors of > 20 than the reported fracture strength level. Breeder cracking, if it occurs, will change the blanket configuration and hence increase the difficulty in predicting breeder performance during operation. The most undesirable effect of cracking appears to be the difficulties created in controlling thermal conductance at the breeder-to-tube interface. Similar to UO_2 and/or $(U,Pu)O_2$ nuclear fuels, Li_2O breeder may fracture into fragments and thus greatly complicate the thermal conductance control. The impact of breeder cracking on the flow characteristics of the helium purge stream is also an important consideration. Of the critical Li_2O properties that affect cracking, fracture strength and Young's modulus, in particular, warrant experimental investigation.

The reference Li_2O breeder first wall/blanket design is illustrated in Figure 2. Major parameters are listed in Table 3. The first wall and blanket are integrated mechanically and structurally into modules, assembled into eight blanket sectors, identical except for local variations required for other reactor components (e.g., REB current drive launcher). The first wall is a beryllium-clad corrugated panel, with channels of circular segment cross section. The breeder and first wall are cooled by high-pressure (11.0 MPa), high-temperature (260°C inlet, 300°C outlet) water. The breeder coolant is contained in small-diameter tubes connected to inlet and outlet manifolds at the rear of the blanket. A stainless steel metallic felt, which accommodates thermal expansion differences between the breeder and tube and conducts the heat from the breeder to the tube is being evaluated for control of the breeder temperature. The Li_2O breeder is fabricated at 70% of theoretical density, with bimodal porosity to enhance tritium release. Helium purge gas at approximately 1 atm flows through 2-mm diameter holes in the breeder to remove tritium. Dual parallel primary coolant loops are provided to effect safe removal of afterheat in the event of a coolant circuit failure. Maintenance of the first wall/blanket is performed by sector removal and replacement, to minimize downtime.

TABLE 3. Li_2O BREEDER REFERENCE FIRST WALL/BLANKET CONCEPT DESCRIPTION

Selected Materials	
-Tritium Breeder	Li_2O (solid; 70% TD)
-Coolant	Press. H_2O (11.0 MPa) - Inlet Temp. 260°C - Outlet Temp. 300°C
-Tritium Proc. Fluid	Low-Vel. He (0.05 Mpa)
-Structure	Modified Austenitic SS
Selected Design Options	
-First Wall	Be-clad Corrugated Panel
-Breeder Coolant Containment	Small-diameter Tubes
-Other:	
-First wall & blanket mechanically & structurally integrated	
-Coolant flow in toroidal direction	
-Dual parallel primary coolant loops	
-Maintenance by sector removal & replacement	

B. Li-Pb alloy blanket concepts

Liquid Li-Pb alloys have several attractive properties for use as a tritium breeder in a fusion reactor, viz., excellent tritium breeding performance and acceptable tritium recovery characteristics. The 17Li-83Pb eutectic alloy, which has a relatively low melting temperature, 235°C, was selected as the reference breeding material for the liquid breeder portion of the DEMO blanket study.

The most important initial consideration for the blanket design is whether to use Li-Pb as both breeder and coolant (i.e., self-cooled), or to use a separate gas or liquid coolant. Economics-related issues (e.g., pumping power losses and energy-conversion-efficiency), safety, and blanket and coolant system design complexity are of primary concern. The most important materials-related concerns pertinent to the design evaluations are: (1) the high density of Li-Pb, which increases blanket structural requirements (and pumping power requirements if used as a coolant); (2) the maximum allowable structural temperature at the liquid metal interface, set at 400°C to 450°C for ferritic steel because of compatibility concerns; and (3) the low solubility of tritium in Li-Pb, which impacts both tritium containment and tritium recovery. For separate coolant concepts, additional important design considerations are breeder-coolant compatibility, control of tritium permeation into the coolant, breeder containment approach, and coolant containment approach (e.g., fully pressurized module or small-diameter coolant tubes). Induced magnetohydrodynamic (MHD) effects are also important concerns for Li-Pb breeder self-cooled concepts and for separately cooled concepts using liquid metal coolant (i.e., sodium).

Helium, pressurized water, and liquid sodium have been considered as potential coolants for the separate-coolant concepts. Sodium, on balance, is considered to be the best separate coolant, primarily because of its good thermal-hydraulic characteristics, its low reactivity with Li-Pb, and its potential to serve as a tritium-recovery medium without requiring Li-Pb circulation. However, MHD effects and reactivity of sodium with water and air are major concerns.

The maximum blanket operating temperature was limited by corrosion/compatibility criteria. Critical issues include (1) corrosion/mass transfer effects and (2) stress corrosion effects. Ferritic steel and vanadium alloys

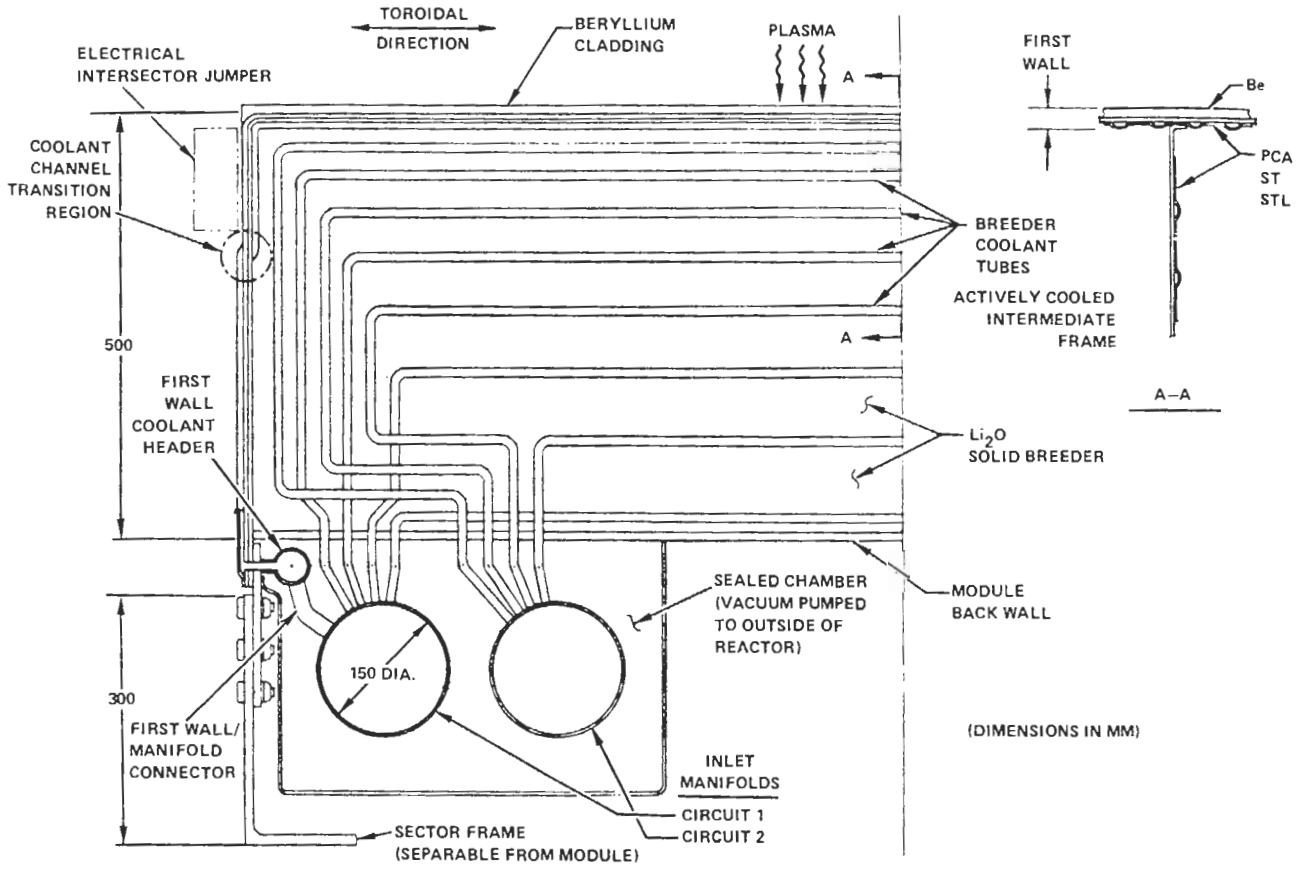

Figure 2. Li_2O solid breeder first wall/blanket design.

are considered to be the best candidates for the structural material. Because of the high solubility of nickel in both lithium and lead, structural alloys containing significant amounts of nickel are subject to extensive mass transfer at high temperatures. Those ferritic steels with no nickel should be more resistant to mass transfer effects; however, liquid metal embrittlement at low temperatures (~ 350°C) is of concern for structures under high stress. Vanadium alloys probably have better compatibility with Li-Pb because of lower solubilities in lithium and lead; however, no experimental data are available. Also, for separately cooled concepts compatibility of structure with the separate coolants is a major consideration.

Neutronics analyses for the Li-Pb breeder blanket indicate that breeding ratios of ~ 1.5-1.6 (1-D basis) are attainable for blankets at 100% coverage and 70-cm depth, depending on first wall materials and thicknesses. However, the Li-Pb must be highly enriched, to ~ 60-70% of ^6Li, to achieve these breeding ratios. A Li-Pb blanket with natural lithium will provide a breeding ratio of only 1.2-1.3 for otherwise similar conditions.

Key properties of 17Li-83Pb that have major impact on the blanket design include its melting temperature (235°C), relatively high density (9.4 g/cm^3), and relatively low solubility for hydrogen (tritium). For a relatively high tritium pressure of 1 Pa, the amount of tritium dissolved in the alloy is only about 4.4 wppb at projected operating temperatures. At this pressure, tritium permeation rates are quite high for most structural materials. The heat of reaction of the 17Li-83Pb alloy with air and water is lower than that of liquid lithium by a factor of ten when compared on a unit volume basis.

Tritium recovery and containment problems were evaluated for both self-cooled and separately cooled concepts. Because of the low solubility of tritium in 17Li-83Pb, fairly high tritium pressures (about 1 Pa) are required to attain acceptable flow rates if Li-Pb is used as the tritium recovery fluid. These high tritium pressures create tritium containment difficulties for self-cooled con-

cepts in the "ex-reactor system", e.g., the steam generator and piping. An intermediate heat exchanger or a double-walled steam generator would be required to reduce leakage of tritium to acceptable levels. Molten salt extraction, the use of solid getters, and gas sparging are considered feasible methods for direct recovery of tritium from Li-Pb. For sodium coolant in the separately cooled concept, permeation rates into the sodium appear to be sufficient to use the sodium as the tritium recovery fluid. Cold-trapping is the most attractive method for recovery of tritium from the sodium.

The sodium-cooled Li-Pb first wall/blanket concept is illustrated in Figure 3; major parameters are listed in Table 4. The module/sector approach used for the Li_2O breeder blanket was adopted for this Li-Pb breeder blanket concept. The first wall and blanket are integrated mechanically and structurally. The first wall consists of a beryllium-clad corrugated panel. The breeder zone and first wall are cooled by low-pressure ($\lesssim$ 1 MPa), high-temperature (275° inlet, 400°C outlet) liquid sodium, contained in small-diameter toroidally oriented tubes which are connected to inlet and outlet manifolds at the rear of the blanket. Tritium permeates from the Li-Pb (which does not circulate out of the modules) through the coolant tube walls into the sodium; a small percentage of the sodium flow is processed externally by cold trapping to remove the tritium.

TABLE 4. DEMO Li-Pb LIQUID METAL ALLOY BREEDER BLANKET DESCRIPTION

Selected Materials	
-Tritium Breeder	Liq. 17Li-83Pb Alloy
-Coolant	Liq. Sodium ($\lesssim$ 1.0 MPa) -Inlet temp. ~275°C -Outlet temp. ~400°C
-Structure	Ferritic Steel or Vanadium Alloy
Selected Design Options	
-First Wall	Be-clad corrugated panel
-Breeder Coolant Containment	Small-diameter tubes
-Other:	
-Toroidal direction for coolant flow	
-Dual parallel primary coolant loops	
-Maintenance by sector removal & replacement	

For the Li-Pb self-cooled first wall/blanket concept, the beryllium-clad first wall of each module is formed by two semi-ellipsoidal domes which comprise the module front face. The flat side walls of the module are connected to full internal frames (oriented normal to the toroidal direction) which self-react loads due to internal pressure (~ 1-2 MPa). The frames also react the gravity loads of the Li-Pb from the side walls and first wall (depending on module location in the sector) to the back wall and sector structure. The Li-Pb enters the rear of the blanket at about 300°C, flows to the front of the blanket through radial feedpipes, and is channeled directly behind the first wall to cool it. The liquid metal then circulates at a lower velocity toward the back of the blanket, and exits at 400°C to the outlet manifold. A fraction of the Li-Pb flow is diverted to an ex-reactor tritium processing system for tritium recovery.

IV. CURRENT DRIVE

This section summarizes results from theoretical studies of a noninductive current drive for DEMO. A lower hybrid (LH) system was previously designed in detail for STARFIRE.[2] The LH system appeared workable from an engineering and maintenance viewpoint, but accessibility constraints on the wave prevented wave penetration to the high-density plasma interior.[4] Hence, a survey of other drivers was conducted in order to identify those which more efficiently generate centrally peaked current density. The goal of our survey is to find which driver maximizes the net electrical power produced by the DEMO.

A large number of external drivers have been proposed which theoretically can sustain the toroidal tokamak current in a steady, noninductive state. Both plasma waves and particle beams have been suggested, and a survey of the most attractive candidates has been performed. We classify waves into three types. High-phase-speed (HS) waves are those which have toroidal phase velocities exceeding the electron thermal speed and which directly impart momentum to the circulating electrons. Examples of these waves, which have received experimental tests for driving current, are the lower-hybrid wave (JFT-2, PLT), the magnetosonic (Synchromak), and the ion-cyclotron wave (Model C). Low-phase-speed (LS) waves are those which have subthermal phase speeds and supply electron momentum. The most studied example is the fast wave, which is the compressional Alfven wave (CAW) at low fre-

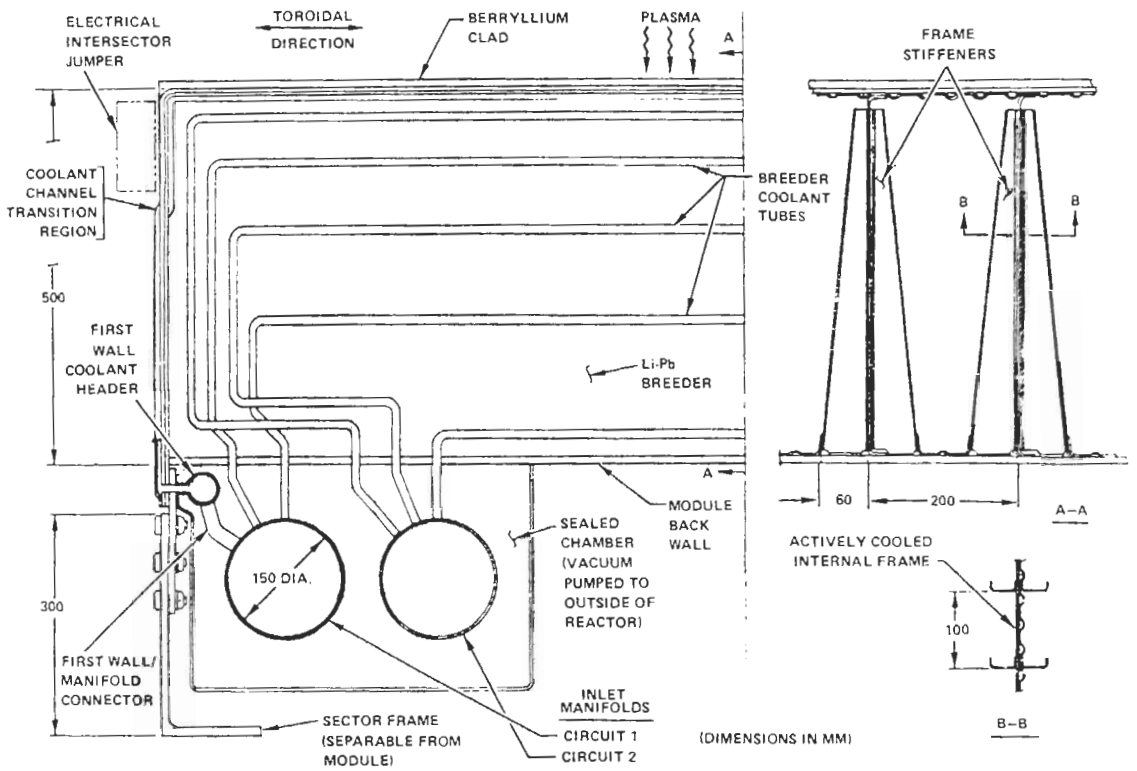

Figure 3. 17Li-83Pb liquid alloy breeder first wall/blanket design.

quencies and which is called a low-speed (short parallel wavelength) magnetosonic wave above the ion cyclotron frequency. The third wave-current-drive classification refers to ICRH and ECRH techniques, which heat plasma to create anisotropic resistivity, thereby indirectly driving currents. Beam-driven currents may be created by injection of neutral beams (DITE) or relativistic electron (REB) beams (SPAC-VI).

Theoretical predictions of the ratio of current density to absorbed driver power density in the plasma were compiled and compared for all these drivers. Details are given in Ref. 5. The DEMO study computed power requirements to generate the full 8.7 MA toroidal current in steady state, assuming a centrally peaked current density, consistent with engineering limitations of the launcher and plasma physics constraints on driver power deposition.

The dominant consideration in the driver survey was the net electric power produced for each driver, since this is the primary goal of a demonstration electric power plant. Results for three drivers are presented in Fig. 4. For this comparison, plasma beta and current are held constant, and both the fusion power, P_f, and driver power, P_d, are computed for different temperature and density combinations. The net electric power, P_n, was estimated by the formula $P_n = 0.36 \times P_f - 22 - (P_d/\eta_d)$, where the units are megawatts. The driver electric power efficiency, η_d, is not known very accurately since these systems are all experimental, but we see that systems vary in their sensitivity to η_d. As an example, consider neutral beams, which require $P_d \tilde{\sim} 100$ MW to maintain the toroidal current in DEMO. Since this is a substantial portion of the gross electric power ($0.36 \times P_f$), the net power is very sensitive to the driver efficiency, η_{NB}. It appears likely that steady-state DEMO is possible with a neutral D° driver, but advanced technology (negative ions, efficient accelerators, photo-neutralizers) would be needed.

At the other extreme, the REB has received relatively little experimental study, but it promises in theory to require power input of only a few times the conventional

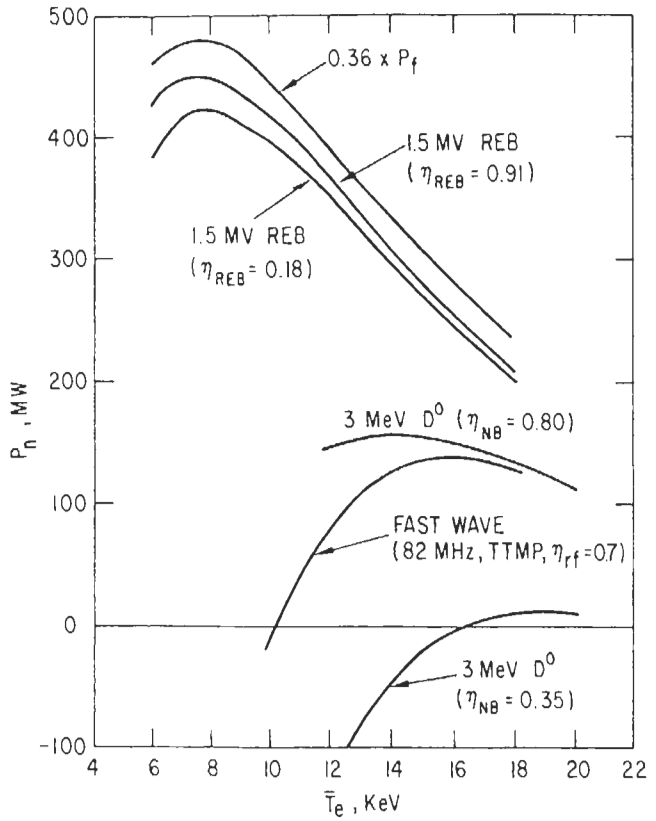

Fig. 4. Gross power (0.36 x P_f) for DEMO and net electric power for three driver candidates: continuous neutral injection (3 MeV D°); continuous fast wave (82 MHz); and pulsed REB (1.5 MeV, 4 MJ per pulse). $\bar{T}_e$ is varied with $\beta \equiv 8\%$; $P_n = (0.36 \times P_f) - 22 - (P_d/n_d)$, in MW.

ohmic heating power, $P_d \lesssim 10$ MW. This power is almost negligible compared to the gross electric output, and, thus, the net power is insensitive to the efficiency η_{REB}, as shown in the figure. Another driver (not shown) is the compressional Alfven wave (CAW) at frequencies less than the ion cyclotron frequency, and this also promises very low circulating power. Ironically, this driver has received virtually no experimental study. Prospects for efficient REB and CAW current drive are confounded by questions regarding the current density profiles which are likely to result in the steady state. If electrons behave neoclassically, there are reasons to suspect that hollow current densities would be obtained. While the stability of hollow current densities has only recently begun to receive theoretical study, it seems likely that centrally peaked current densities will allow stable operation at higher betas.

The lower hybrid (LH) wave has been the most successful experimental driver, but it may fail to simultaneously satisfy the DEMO requirements of substantial net power, centrally peaked current density, and purely steady-state plasma operation. The reason for this is that the wave requires slow phase speeds (large parallel index of refraction, $n_\parallel$) to be accessible to the high density central region. In consequence, in order to generate centrally peaked current density, the driver efficiency is quite small; values of $P_{LH} \gg 50$ MW are predicted for DEMO. One solution to this circulating power limitation would be to operate DEMO in a mode in which the plasma density (and resistivity) are periodically cycled. The relative costs and benefits of this operating mode were not addressed in the present study but are under study.

At frequencies above the ion cyclotron frequency, the fast wave can be a relatively efficient driver. This high-phase-speed magnetosonic wave (HSMS) has no accessibility limitation, so $n_\parallel$ is not limited by wave reflection. However, if $n_\parallel$ is close to unity, ion cyclotron damping competes with electron transit time magnetic pumping (TTMP), reducing current drive efficiency. Results for single-pass absorption in DEMO are shown in the figure. Unfortunately, this driver has not yet received experimental tests in collisionless tokamaks.

Reactor availability is another crucial factor to a DEMO power plant. From this point of view, the neutral beam driver would be a particularly poor choice since it is physically quite large and requires a line of sight to the plasma. These features combine to hinder access to the reactor, which results in long down times for reactor maintenance. In contrast, the REB and wave drivers have power transmission lines which are easily routed around corners. Additionally, these latter drivers permit the location of primary power sources in a room distant from the reactor hall, so hands-on maintenance of the sources is permissible, possibly even during reactor operation.

ACKNOWLEDGMENTS

This paper summarizes the results of a study which incorporates the contribution of many fusion physicists and engineers from several institutions. Ref. 1 should be consulted for a complete list of contributions.

REFERENCES

1. M. A. ABDOU, et al., "A Demonstration Tokamak Power Plant Study (DEMO, final report)," Argonne National Laboratory, ANL/FPP-82-1 (September 1982).

2. C. C. BAKER, et al., "STARFIRE - A Commercial Fusion Tokamak Power Plant Study," Argonne National Laboratory, ANL/FPP-80-1 (September 1980).

3. "International Tokamak Reactor - Phase 2A," International Atomic Energy Agency, Vienna (to be published).

4. D. EHST, et al., J. Fusion Energy, 2 83 (1982).

5. M. A. ABDOU, et al., "A Demonstration Tokamak Power Plant Study (DEMO), Interim Report," Argonne National Laboratory, ANL/FPP/TM-154 (January 1982).